REMARKS

Reconsideration is respectfully requested. Claims 1-4 and 10 are present in the application. Claim 2 is amended herein. Non-elected claims 5-9 were canceled previously.

Claims 1-4 and 10 are rejected under 35 U.S.C. §112, first paragraph, as allegedly failing to comply with the enablement requirement. Applicants respectfully traverse.

The Examiner asserts that the concept of the first internal stress and the etching stop layer having a lower internal stress than the first internal stress, is not supported by the specification. While the Examiner does note that page 11 line 18 to page 12, line 4 of the English specification teaches the following:

> The etching stop layer 7 used in the present invention functions as an etching stop layer during the dry-etching of the front-side silicon membrane 2. The etching stop layer 7 is made of a material which provides a lower internal stress to the etching stop layer 7 after formed, i.e. one selected from a group consisting of Cr, Ti, Ta, Mo, W, and Zr and nitrides, oxides, and oxynitrides of these metals.
>
> The internal stress of the etching stop layer 7 for preventing the deformation of the silicon membrane 2 is preferably in a range from -10 MPa to +10 MPa. Minus "-" represents the compression stress and plus "+" represents the tensile stress.
>
> The thickness of the etching stop layer 7 is in order of 100 nm to 1 μm and can be formed by way of sputtering technique or CVD technique so as to control its stress.

The Examiner asserts that this is not sufficient to enable one skilled in the art to practice the invention.

Applicants respectfully assert that the disclosure is enabling. That is, it is a well-known technique that film stress can be controlled by adjusting gas pressure and the like in a sputtering method (see attached reference material 4, Japanese patent 2,613,646, granted Feb. 27, 1997, FIG. 6 for example).

A partial translation of that document is as follows:

> FIG. 6 shows a relationship between a sputtering gas pressure of Xe and a Ta film stress when a Ta film with a thickness of 0.7 μm is formed by using Xe gas as sputtering gas at a substrate temperature of 200°C, a high frequency output of 660 W, and a substrate bias potential in a floating state (+6 to +7 V).

While it is noted that with respect to a sputtering condition that stress of a stop layer becomes from -10 Mpa to +10 Mpa is not described in the present invention, nevertheless, an optimum value of the sputtering condition (gas pressure and the like) becomes different depending on a sputtering device and mask size, therefore a numerical value itself has no meaning. As long as the fact that stress of film formation changes by changing gas pressure and the like is known, the optimum value can be obtained by optimization operation.

Therefore, it is understood that a detailed numerical value for the condition is not necessary.

In fact, such detailed numerical value is not included in the HOYA cited reference, EP 1 065 566 (Hoya Corporation).

By definition, internal stress is not determined only by materials, and significantly varies depending on film forming method and the like.

In general, a film with low stress is obtained by utilizing this nature of varying internal stress.

In view of the above, it is respectfully submitted that the specification is enabling and withdrawal of the rejection under section 112, first paragraph, is respectfully requested.

Claims 1-4 and 10 are rejected under 35 U.S.C. §102(b) as allegedly being anticipated by or under 35 U.S.C. §103(a) as being obvious over Hoya, EP 1 065 566. Applicants respectfully traverse.

The Examiner states that he is unable to discern any significant difference between the applicant's claimed invention and the Hoya Corporation reference, and that the burden is on the applicant to show the difference. On page 6 of the office action, the Examiner puts FIG. 3 of the applicant's drawings next to FIG. 15 of Hoya's drawings, and states that layer 55 appears to be much the same as layer 39 of applicant's. While it was submitted before to the Examiner that Hoya's layer 55 would not meet the language of the claims of having lower internal stress than said first internal stress, the Examiner seems unpersuaded.

Applicants respectfully assert differences between the present invention and the HOYA cited reference.

Aspects of the present invention are:

1. In manufacturing of an EPL mask (stencil mask, through type mask), an etching stop layer is essential in order to carry out etching with high precision. (A desired shape is not obtained.)

2. Provided, however, that in a method that uses a conventional BOX layer (intermediate oxide film layer) as the etching stop layer, positional accuracy cannot be maintained due to variation of stress before and after pattern formation.

3. In view of the above, the present invention attempts to remove the BOX layer having high compressing stress, and (takes trouble to) provide a stop layer having low stress in place thereof (in order to achieve the object, steps rather become complicated).

4. Objects of using the stop layer are limited to the following:

(i) Used as a stop layer at the time of etching (acting as a cover to prevent etching gas and reactant gas from leaking); and

(ii) Preventing generation of position aberration due to stress change between before and after the pattern formation (existence or nonexistence of the stop layer).

Therefore, the stop layer is removed at the time a mask is used (unnecessary material).

With respect to this point, the present invention is significantly different from a scatterer supporting layer of the

HOYA invention (SCALPEL mask, membrane mask, and scattering-type mask).

This point is described in Exhibit 2, attached, which answers the questions raised by the Examiner in page 6 of the office action.

Therefore, applicants respectfully submit that the rejection of applicants' claims as being identical to the SCALPEL mask are not sustainable.

Materials (Cr, Ta, Mo, W, and Zr, and nitrides, oxides, and oxynitrides of these metals) of the stop layer in claim 2 are different from the materials of a pattern supporting layer in Hoya. Therefore, claim 2 is patentable.

In light of the above noted amendments and remarks, this application is believed in condition for allowance and notice thereof is respectfully solicited. The Examiner is asked to contact applicant's attorney at 503-224-0115 if there are any questions.

It is believed that no further fees are due with this filing or that the required fees are being submitted herewith. However, if additional fees are required to keep the application pending, please charge deposit account 503036. If fee refund is owed, please refund to deposit account 503036.

Respectfully submitted,

James H. Walters, Reg. No. 35,731

Customer number 802
patenttm.us
P.O. Box 82788
Portland, Oregon 97282-0788 US
(503) 224-0115
DOCKET: A-468

Certification of Electronic Transmission

I hereby certify that this correspondence is being electronically transmitted via EFS to the Patent and Trademark Office on this December 17, 2007.

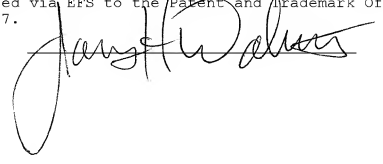

Exhibit 2

Response to Question of the Examiner (Office Action Page 6)

Reference document 3

Yamashita, J.Vac.Sci.Technol.B 18(6), pp. 3237(2000)

Document about the SCALPEL mask and SCALPEL system

I. In INTRODUCTION, there is description with respect to a comparison (difference, advantage, disadvantage) between the SCALPEL mask and the stencil mask.

FIG. 1 shows a comparison between (a) SCALPEL mask and (b) stencil mask.

FIG. 2 shows a comparison between (a) SCALPEL system and (b) EB stepper system

Mainly (refer to TABLE 1),

Stencil mask: has good resolution; however, an isolated pattern is not available (mask division and overlay exposure are necessary)

SCALPEL mask: has inferior resolution; however, an isolated pattern is available (no restriction on patterns)

IV. In MEMBRANE PREPARATION, there is description about stress control.

The description merely describes that "film stress is controlled by process conditions (film forming speed, temperature process, and the like)".

- Although the present invention also does not describe details of the sputtering conditions, we believe this does not lead to insufficient disclosure.

The HOYA cited reference is about a blank of the SCALPEL mask. On the other hand, the present invention is about a blank of the stencil mask.

The SCALPEL mask includes a pattern supporting layer 55, and therefore can be provided with an isolated pattern. However, in order to support an electron beam scattering layer 52 against gravity, the pattern supporting layer 55 has suitable tension stress (FIG. 1).

On the other hand, in the stencil mask, a pattern layer (silicon thin film layer 32) itself is a self-holding film, therefore an etching stop layer 39 does not need to have a function to support the pattern layer (that is, the suitable tension stress is not necessary).

Provided, however, that since it is the stencil mask (since it is through-type), the etching stop layer needs to be removed by when it is completed as a mask. Then, it is necessary to prevent a position of a pattern from changing between existence and nonexistence (before and after the removal) of the etching stop layer.

Nevertheless, it has been difficult to reduce the fluctuation of the position of the pattern in a conventional method of utilizing a silicon oxide film as the etching stop layer. This is because the silicon oxide film has high compressing stress (FIG. 3).

In view of the above, in the present invention, the silicon oxide film is removed, and an etching stop layer having low stress is provided in place thereof, thereby resolving the problem (FIG. 2).

FIG. 2. Stencil Mask/Blank of Present Invention

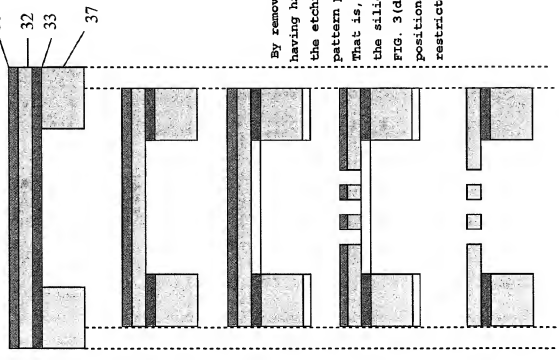

FIG. 3 Conventional Stencil Mask/Blank

FIG.5(c)

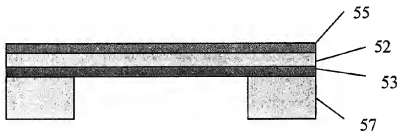

FIG.5(d)

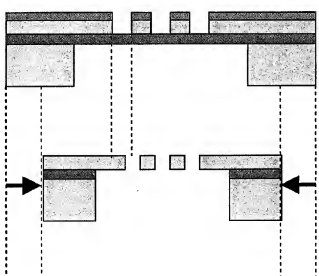

FIG.5(e)

By removing the silicon oxide film layer (53) having high compressing stress, the silicon thin film layer (= pattern layer) (52) is released and is deformed in a contracting manner, and therefore positional accuracy of the pattern cannot be maintained.

That is, the pattern position changes between before and after pattern formation.

FIG. 1. Reasons for Considering Pattern Supporting Layer 55 of Hoya Cited Reference is Tension Stress

FIG.15G

Reference data 3

High-performance membrane mask for electron projection lithography

Hiroshi Yamashita[a)]
ULSI Device Development Laboratory, NEC Corporation, 1120 Shimokuzawa, Sagamihara, Kanagawa 229-1198, Japan

Isao Amemiya
R&D Center, HOYA Corporation, 3280 Nakamaru, Nagasaka, Kitakoma, Yamanashi 408-8550, Japan

Eiichi Nomura
Fundamental Research Laboratories, NEC Corporation, 34 Miyukigaoka, Tsukuba, Ibaraki 305-8501, Japan

Ken Nakajima and Hiroshi Nozue
ULSI Device Development Laboratory, NEC Corporation, 1120 Shimokuzawa, Sagamihara, Kanagawa 229-1198, Japan

(Received 1 June 2000; accepted 25 August 2000)

A high-performance membrane mask for electron projection lithography (EPL) systems is proposed. The design and material selection of the mask described here were carefully executed by considering not only the lithographic performance but also various properties. The mask described in this article consists of a 600-nm-thick diamond-like carbon (DLC) scatter on a DLC membrane 30–60 nm thick. The optimum thicknesses are obtained by calculating angular distributions of the transmitted electrons by our in-house Monte Carlo simulator. It is expected to have an electron transmission of up to 80% and a beam contrast of 100% with an appropriate limiting aperture. A 1-mm-sq membrane of thickness of down to 30 nm could be successfully prepared. The high-performance membrane mask can obtain high resolution and high throughput of the EPL systems simultaneously. © *2000 American Vacuum Society.* [S0734-211X(00)08306-2]

I. INTRODUCTION

The electron-beam (EB) scattering mask is an indispensable key technology for electron projection lithography (EPL), such as the scattering with angular limitation in projection electron-beam lithography (SCALPEL)[1] and the projection exposure with variable axis immersion lenses (PREVAIL)[2] (EB stepper). Two types of mask, the membrane and the stencil, have been proposed (Fig. 1). The SCALPEL membrane mask consists of three layers of thin films: typically a 150-nm-thick SiN membrane, a 10-nm-thick Cr etching stopper, and a 50-nm-thick W scatterer.[3,4] The stencil mask consists of a 2-μm-thick Si scatterer with openings.[5] Each of these masks has merits and demerits (Fig. 2 and Table I). For instance, energy loss due to inelastic scattering in the membrane may result in chromatic aberration and degrade the lithographic resolution. The stencil mask has pattern restriction that must be split into complementary masks, causing reduction of throughput by multiple exposures. Thus, performance of an EB scattering mask affects the resolution and throughput of EPL systems.

In this article we describe a high-performance membrane mask for EPL systems, one maximizing resolution as well as throughput. First, the mask design approach and the energy distribution of the mask-transmitted electrons are discussed. After the material selection is discussed, how the optimum mask structure was designed by using electron scattering simulations is explained. Finally, the extremely thin prepared membrane is shown.

II. CONCEPT OF HIGH-PERFORMANCE MEMBRANE MASK

A. Mask properties

We chose the membrane-type mask because the stencil-type mask has pattern restrictions or needs a mask split which seems to be the most critical issue in using the mask.

As a primary function, a mask has to produce scattering contrast sufficient for fine pattern transfer. From this requirement, the optimum scatterer thickness of the selected material is determined under given optics conditions. As physical properties, a mask should have high mechanical strength for self-supporting, and high electrical and high thermal conductivities to relieve the mask from charging[6] and heating. As chemical properties, a mask should have high acid resistance for mask cleaning and high etching profile controllability for linewidth accuracy. In addition, mask stability to EB radiation is also required. From these requirements, the membrane and scatterer materials are selected and the mask structure is designed.

The preferable membrane will be made of a low density material and made as thin as possible for less electron scattering. On the other hand, the preferable scatterer will be also made of a low density material but rather thick so that it has mechanical strength sufficient for self-supporting. The proposed membrane mask takes the merits of both the mem-

a)Electronic mail: h-yamashita@df.jp.nec.com

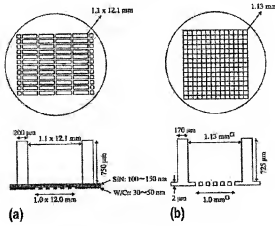

FIG. 1. Schematic diagram of two types of masks for electron projection lithography: (a) SCALPEL mask and (b) stencil mask.

brane and stencil-type masks, that is, the membrane supports only the unsupported, unstable, or fragile scatterer features.

B. Energy distribution

Energy distribution of the mask-transmitted electrons is very important because an energy spread, ΔE, due to the inelastic scattering in a membrane may result in chromatic aberration and degrade the resolution of exposure systems. Because of this, the beam semi angle, α, will be limited and the energy loss affects not only the resolution but also the throughput. Particularly, a plasmon loss near zero loss characterizes the energy distribution of the mask-transmitted electrons. More strictly, the number of electrons at and around the plasmon loss is very important. We can increase the beam semiangle and the beam current by reducing the intensity of the plasmon loss. Therefore, is very important to investigate the energy distribution because it assesses membrane performance and may determine the thickness. To this end, we conducted Monte Carlo simulations and direct measurements of the energy distribution of the mask-transmitted electrons. The experimental results will be presented elsewhere.

TABLE I. Comparison of masks for EPL systems.

Parameters	LOTUS	SCALPEL	STENCIL
Mask type	DLC membrane	SiN membrane	Si stencil
Structure	DLC/Si/DLC	W/Cr/SiN	Si/opening
Membrane thickness	30–60 nm	100–150 nm	...
Beam transmission	70%–80%	30%–40%	100%
Energy spread by mask	Approx 20 eV	Approx 22 eV	0 eV
Scatterer thickness	600 nm	30–50 nm	2 μm
Mask split	Unnecessary	Unnecessary	Necessary

When the membrane thickness is much greater than the mean free path under a given condition, the continuous slowing down approximation (CSDA) can be used to calculate the energy distribution. When the thickness is comparable to the mean free path, however, elementary process models for the inelastic electron scattering events have to be used to calculate it. We used a commercially available Monte Carlo simulator, VS-M/EB, from Fuji Research Institute Corporation. In the electron-scattering simulation, the following four elementary processes are adopted: inner-shell electron excitation, valence electron excitation, conduction electron excitation, and plasmon excitation.[7]

The energy distributions calculated for 150- and 30-nm-thick Si membranes are shown in Fig. 3. By reducing the membrane thickness, the intensity of zero loss, I_{zero}, becomes large and that of the first plasmon loss, I_{p1}, becomes small. In the case in which Si membrane thickness is reduced from 150 to 30 nm, the I_{zero} increases from 31.5% to 76.9% (the percentage to the total incident electron number, 50 000), and the I_{p1} decreases from 2.1% (6.7% of the I_{zero}) to 1.0% (1.3% of the I_{zero}). The intensity of the first plasmon energy loss relative to that of zero loss (I_{p1}/I_{zero}) becomes 1/5. This intensity reduction allows the use of a large beam semiangle and improves the resolution and throughput of the EPL systems. The thinner membrane is better in terms of the electron transmission and the energy spread.

III. MASK STRUCTURE DESIGN

A. Calculation of angular distribution

To determine the optimum thickness of the membrane and scatterer, we calculated the angular distributions of the mask-

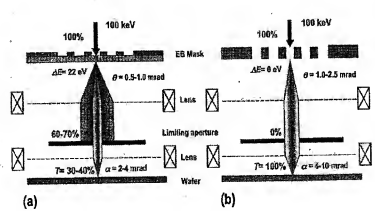

FIG. 2. Schematic comparison of masks in 100 kV electron projection lithography systems: (a) SCALPEL and (b) EB stepper.

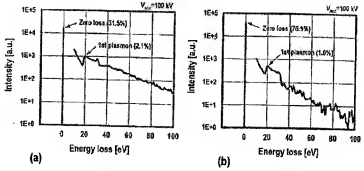

FIG. 3. Energy distributions calculated for Si membranes (a) 150 and (b) 30 nm thick.

transmitted electrons by using the in-house Monte Carlo simulator we previously used in analysis of cell-projection masks.[8–10] A screened Rutherford scattering cross section was used as an elastic scattering model. The electron scattering for various materials for the SCALPEL mask was investigated in detail and reported by Mkrtchyan *et al.*[11] In our simulations, we used Si as the material for the membrane and scatterer because it has a low density and has been a standard material for EB masks.[9–11] Figure 4 shows the cumulative electron transmission, T (%), as a function of aperture semiangle, θ (mrad), for various thickness of Si, t (nm), under an accelerating voltage, V_{acc}, of 100 kV. The transmission is a percentage to the irradiated electron number.

Figure 5 shows the transmission as a function of Si thickness when the aperture semiangle is 2 mrad, which corresponds to a beam semiangle of 8 mrad at the wafer for 4× optics. The change in the transmission is monotonous in an aperture semiangle range from 0 to 5 mrad as shown in Fig. 4. The transmission decreases with increasing Si thickness and becomes almost zero when the thickness is 600 nm. A thinner membrane is obviously better in terms of electron transmission, but the mask fabrication process must be taken into account when determining the optimum membrane thickness.

B. Material selection

We evaluated various membrane materials, such as B-doped Si, diamond-like carbon (DLC), and SiC. The optional intermediate layer (5–10 nm thick) would be an etching stopper made of a material such as amorphous Si, SiC, Ti or $TiCrN_x$. And the top layer must be a rather thick scatterer made of a material such as Si or DLC.

We sought the best material by using the flexural rigidity to evaluate mechanical strength. The flexural rigidity of a square film supported on four sides can be designated D and given by

$$D = Et^3/12(1-\nu^2), \tag{1}$$

where E is the Young's modulus, t is the film thickness, and ν is the Poisson ratio. Here, we define Et^3 as the self-supporting index, $\sigma_{m,s}$, for a membrane at $t_m = \Lambda/3$, where the transmission, $T_m = \exp(-1/3) = 72\%$,

$$\sigma_m = Et_m^3 = E(\Lambda/3)^3, \tag{2}$$

and for a scatterer at $t_s = 3\Lambda$, where $T_s = \exp(-3) = 5\%$,

$$\sigma_s = Et_s^3 = E(3\Lambda)^3. \tag{3}$$

Λ is an elastic scattering mean free path under the given conditions. The Poisson ratio is negligible because its square

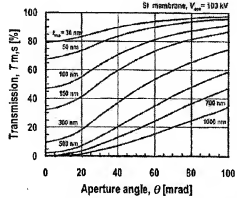

FIG. 4. Angular distributions calculated for various thicknesses of Si.

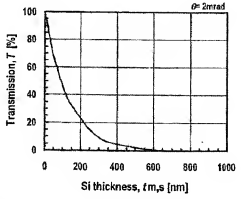

FIG. 5. Cumulative electron transmission as a function of Si thickness when the aperture semiangle is 2 mrad.

TABLE II. Typical material properties.

Material	Young's modulus E (GPa)	Poisson's ratio ν	Density ρ (g/cm^3)	MFP Λ(nm)	Self-supporting index (pN m) σ_m	σ_s
DLC	130–300		2.1–2.8	125–165	9.4–51	6800–37 000
SiN_x	130–160	0.24	3.19	110	6.4–7.9	4600–5700
SiC	260–300	0.14	3.17	110	13–15	9400–11 000
W	350	0.29	19.4	18	0.076	55
Ta (TaGe)	160–190	0.35	16.1	22	0.063–0.075	44–52
Si (100)	130	0.44	2.33	150	16	12 000
Diamond	450–500		3.52	100	17–33	12 000–24 000

is very small. The self-supporting index is given by the mask structure and the material used. The mean free path (MFP) is calculated using a density assuming that the MFP of Si is 150 nm at 100 kV. Typical material properties and the self-supporting indexes are listed in Table II. DLC film grows in the Frank–van der Merwe (monolayer) growth. So it is the only one of these materials that can be an extremely thin membrane, and others grow in Volmer–Weber (nucleation) growth. Heavy metals such as W and Ta have great scattering ability, but their mechanical strength is less than that of the other materials. A DLC scatterer, on the other hand, is strong enough to be self-supporting. We therefore selected DLC as the best material for both the membrane and the scatterer. The electrical conductivity of a DLC scatterer can be increased by doping, so an additional conductive layer is not necessary. As a suitable material for the etching stopper, amorphous Si can be used.

C. Optimum mask structure

The density of DLC is close to that of Si, so that the result shown in Fig. 4 can be used to estimate the optimum thickness. With regard to the scatterer thickness, the minimum and optimum thickness is 600 nm in terms of the beam contrast, C, on the wafer. If the scatterer is less than 600 nm thick, the contrast decreases. And if it is thicker than this, it becomes heavy and loads the membrane with unself-supported features such as the doughnut pattern. With the optimum mask structure, electron transmission of up to 80% and beam contrast of 100% can be expected with an appropriate limiting aperture. The rather thick scatterer, but much thinner than the Si stencil mask with a low density material gives high mechanical strength to the mask. The properties of the proposed mask, light on the ultimate (EPL) system (LOTUS), are listed in Table I.

IV. MEMBRANE PREPARATION

The three-layer high-performance membrane mask described here can be prepared by chemical vapor deposition (CVD) or sputtering processes. Extremely thin membranes 1 mm square down to 30 nm thick were successfully prepared by using a CVD process, shown in Figs. 6(a) without and 6(b) with stress control. The film stress was controlled by process conditions such as deposition rate and thermal treatment. The Young's modulus and the density of the stress-controlled membrane were measured to be 170 GPa and 2.4 g/cm^3, respectively, and the self-supporting index is estimated to be 20 pN m. This thickness is equivalent to 22 nm of a SCALPEL SiN membrane in terms of the electron transmission. It is well known that DLC films may be prone to radiation damage due to hydrogen content. Therefore, the hydrogen density should be less than 10 at. %. The membrane preparation process will be presented elsewhere. We will pursue exposure experiments using the proposed mask. The results will be also reported in a later publication.

V. CONCLUSIONS

We designed a high-performance membrane mask for electron projection lithography. It consists of a 600-nm-thick diamond-like carbon scatterer on a DLC membrane 30–60

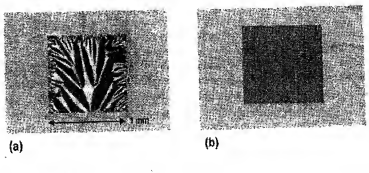

FIG. 6. Optical microscope photographs of a 30-nm-thick DLC membrane prepared by CVD: (a) without and (b) with stress control.

um thick. A 1-mm-sq membrane down to 30 nm thickness could be successfully prepared. Electron transmission of 80% and beam contrast of 100% can be expected with an appropriate limiting aperture. By reducing the membrane thickness, the intensity of the zero-loss electrons will be increased and the first plasmon loss will be reduced. This will allow the use of a large beam semiangle and as a result improve the resolution and throughput of the exposure systems simultaneously. The high-performance membrane mask will shed light on ultimate EPL systems.

ACKNOWLEDGMENTS

The authors would like to thank H. Hayashi of Fuji Research Institute Corporation for the calculation of energy distribution. They also thank Dr. K. Kasama for his encouragement.

[1]S. D. Berger and J. M. Gibson, Appl. Phys. Lett. **57**, 153 (1990).
[2]H. C. Pfeiffer, Jpn. J. Appl. Phys., Part 1 **34**, 6658 (1995).
[3]J. A. Liddle, H A. Huggins, S. D. Berger, J. M. Gibson, G. Weber, R. Kola, and C. W. Jurgensen, J. Vac. Sci. Technol. B 9, 3000 (1991).
[4]J. A. Liddle, H. A. Huggins, and G. P. Watson, J. Vac. Sci. Technol. B **13**, 2483 (1995).
[5]S. Kawata, N. Katakura, S. Takahashi, and K. Uchikawa, J. Vac. Sci. Technol. B **17**, 2864 (1999).
[6]M. Mkrtchyan, A. Gasparyan, K. Mkhoyan, A. Liddle, A. Novembre, and D. Muller, Microelectron. Eng. **46**, 223 (1999).
[7]K. Fujita, Fuji-ric J. Supercomput. Technol. **5**, 61 (1995) (in Japanese).
[8]H. Yamashita, E. Nomura, E. Ema, K. Itoh, and H. Nozue, J. Vac. Sci. Technol. B **14**, 3845 (1996).
[9]H. Yamashita, E. Nomura, and H. Nozue, J. Vac. Sci. Technol. B **15**, 2263 (1997).
[10]H. Yamashita, V. S. H. Wen, A. R. Neureuther, and E. Nomura, J. Vac. Sci. Technol. B **16**, 3227 (1998).
[11]M. M. Mkrtchyan, J. A. Liddle, A. E. Novembre, W. K. Waskiewicz, G. P. Watson, L. R. Harriott, and D. A. Muller, J. Vac. Sci. Technol. B **16**, 3385 (1998).

Partial translations of the Reference data 4

(1) (11) Patent No. 2,613,646

(24) Date of Grant, Feb. 27, 1997

(2) FIG. 6 shows a relationship between a sputtering gas pressure of Xe and a Ta film stress when a Ta film with a thickness of 0.7 μm is formed by using Xe gas as sputtering gas at a substrate temperature of 200°C, a high frequency output of 660 W, and a substrate bias potential in a floating state (+6 to +7 V).

Reference data 4

(1)

(19)日本国特許庁（ＪＰ）　(12)特　許　公　報（Ｂ２）　(11)特許番号　第2613646号

(45)発行日　平成９年(1997)５月28日　(24)登録日　平成９年(1997)２月27日

(51)Int.Cl.[5]	識別記号	庁内整理番号	ＦＩ	技術表示箇所
Ｃ２３Ｃ　14/22			Ｃ２３Ｃ　14/22	
14/50			14/50	Ｚ

請求項の数３（全　５　頁）

(21)出願番号　特願昭63－321556

(22)出願日　昭和63年(1988)12月20日

(65)公開番号　特開平2－166268

(43)公開日　平成２年(1990)６月26日

(73)特許権者　999999999
大日本印刷株式会社
東京都新宿区市谷加賀町１丁目１番１号

(72)発明者　飯村　幸夫
東京都新宿区市谷加賀町１丁目１番１号
大日本印刷株式会社内

(74)代理人　弁理士　曾井　英雄　（外５名）

審査官　鈴木　正紀

(54)【発明の名称】　低応力金属薄膜の形成方法

(57)【特許請求の範囲】

【請求項１】低応力金属薄膜を形成しようとする基板の表面の外周囲のほぼ全体を導電材からなる基板ホルダに接触させ、さらに当該基板ホルダに所定の基板バイアス電位を付与するとともに、ガス圧力、電力および基板温度を調整してスパッタ法により低応力金属薄膜を形成する方法において、前記基板ホルダの基板外の外周囲部分の面積を前記基板の表面の面積と同程度かまたはそれよりも大きくしたことを特徴とする低応力金属薄膜の形成方法。

【請求項２】前記低応力金属薄膜が、高融点金属または高融点合金を主成分とすることを特徴とする請求項１記載の低応力金属薄膜の形成方法。

【請求項３】前記高融点金属または高融点合金が、モリブデン、タンタル、タングステン、またはタングステン－チタン合金であることを特徴とする請求項２記載の低応力金属薄膜の形成方法。

【発明の詳細な説明】

【産業上の利用分野】

本発明は、バイアススパッタ法を用いた低応力金属薄膜の形成方法に係り、特に半導体集積回路の電極パターン、Ｘ線露光用マスクの吸収体パターン等に用いて好適な低応力金属薄膜の形成方法に関するものである。

【従来の技術およびその課題】

従来行われているバイアススパッタ法を用いた低応力金属膜の形成方法を、第５図乃至第７図に基づいて説明する。

ここで、第５図（ａ）はスパッタ装置の一構成例を示す概念図、第５図（ｂ）は当該装置における基板と基板ホルダとの関係を示す図、第６図及び第７図はそれぞれ

当該装置を用いてTa膜を形成したときの特性を表した図である。

第５図（ａ）において、真空槽21内には、例えばタンタル（Ta）のような金属ターゲット22と、当該金属ターゲット22の薄膜を形成しようとする基板23とが適当な間隔をおいて平行に対峙するように配置されている。上記金属ターゲット22には、スパッタ高周波電源27（13.57MHz）が同調コンデンサ29を介して接続されている。また、上記基板23は、当該基板23の表面外周が基板ホルダ24と接触するようにして当該基板ホルダ24と背板25との間に挟持されている。当該基板ホルダ24は、アルミニウム、ステンレススチール、モリブデン等の導電材で形成されており、基板バイアス電源28に切り替えスイッチ33を介して電気的に接続されている。さらに前記背板25は、加熱ヒータ32が埋め込まれたステンレススチール等からなるテーブル31上に載置されている。なお、この例では、金属ターゲット22の直上に複数の固定磁石30を配置しており、また、バルブ26を介して真空槽21内にスパッタガスを供給するようにしている。

第５図（ｂ）に、第５図（ａ）に示した装置における基板23と基板ホルダ24との関係を詳細に示す。このような従来の装置においては、当該基板ホルダ24の外径2bは、基板ホルダ24の内径2a（これは基板23の表面のうち、スパッタによる金属ターゲット22の薄膜を形成する部分の直径に同じ）より少し大きいだけであった。具体的な一例として、基板23の外径が76mmの場合、2a＝74mm、2b＝83mmで、基板ホルダ24の外周部分の表（おもて）面の面積は基板23のスパッタされる部分の面積の0.26倍でしかない。

(2)

次にこのような装置を用いてTa膜を形成した場合の特性を第６図および第７図に基づいて説明する。第６図は、スパッタガスとしてXeガスを用い、基板温度200℃、高周波出力660W、基板バイアス電位が浮動状態（＋６～＋７V）で0.7μm厚のTa膜を形成した際のXeのスパッタガス圧力とTa膜応力の関係を示している。また、第７図は、Xeガス圧力0.37Pa、基板温度200℃、高周波出力660Wで0.7μm厚のTa膜を形成した際の、基板直流バイアス電位とTa膜応力の関係を示している。

第６図から、Ta膜応力ゼロ近辺でのスパッタ圧力変化量±0.01Paに対するTa膜応力の変化量を見てみると、±2.5×10^8dyn/cm^{2}であり、同程度の再現性があった。ここで、膜応力は、正の値は引張り応力、負の値は圧縮応力であることを示す。第７図から基板直流バイアス電位が0V以下では、Ta膜の応力が急激に圧縮応力となり、不適切であることが分かった。

しかしながら、例えば高精度なX線露光用マスクの吸収体用金属薄膜のように、低応力が要求される場合の膜応力は２$\times10^8$dyn/cm^{2}以下であり、従来の方法ではこれを実現させることは極めて困難であった。

本発明は、上記の課題を解決するものであって、スパッタ法により、従来極めて困難であった低応力の金属薄膜を形成できるとともに金属薄膜の応力を高精度に制御することができる低応力金属薄膜の形成方法を提供することを目的とするものである。

［課題を解決するための手段］

上記の目的を達成するために、本発明の低応力金属薄膜の形成方法は、低応力金属薄膜を形成しようとする基板の表面の外周囲のほぼ全体を導電材からなる基板ホルダに接触させ、さらに当該基板ホルダに所定の基板バイアス電位を付与するとともに、ガス圧力、電力および基板温度を調整してスパッタ法により低応力金属薄膜を形成する方法において、前記基板ホルダの基板外の外周囲部分の面積を前記基板の表面の面積と同程度かまたはそれよりも大きくしたことを特徴とするものである。

［作用および発明の効果］

本発明の低応力金属薄膜の形成方法は、基板ホルダの基板外の外周囲部分の面積を大きくして、形成中の金属薄膜表面に基板直流バイアス電位をより安定に付与できるようにしているため、金属薄膜の膜応力をゼロ近辺の低応力範囲で高精度に制御しながら形成することが可能となる。

［実施例］

以下、図面を参照しながら本発明の好適な実施例について詳細に説明する。

第１図（ａ）は、本発明の低応力金属薄膜の形成方法に適用して好適なスパッタ装置の一実施例構成を説明するための図、第１図（ｂ）は、当該装置における基板と基板ホルダとの関係を説明するための図、第２図乃至第４図は、本発明の低応力金属薄膜の形成方法における各種特性線図である。

図中、１は真空槽、２は金属ターゲット、３は基板、４は基板ホルダ、５は背板、６はバルブ、７はスパッタ高周波電源、８は基板バイアス直流電源、９は同調コンデンサ、10は固定磁石、11はテーブル、12は加熱ヒータ、13は切り替えスイッチである。

まず第１図（ａ）のスパッタ装置は、基板ホルダ４と背板５とを除くと、従来技術の説明に用いた第５図（ａ）と同様の構成になっている。すなわち、真空槽１内には、金属ターゲット２と、当該金属ターゲット２の薄膜を形成しようとする基板３とが適当な間隔をおいて平行に対峙するように配置されている。ここで、上記基板３としては、SiウエハまたはそのほかにSiN、SiC、SiO_2薄膜等が全面または一部に形成されたものを適用することができ、また、上記金属ターゲット２としてはAl、およびそのCu、Si等との合金、またはMo、W、Ta、Tiなどの高融点金属もしくはそれらの合金を適用することができる。上記金属ターゲット２には、スパッタ高周波電源（13.57MHz）７が同調コンデンサ９を介して接続されている。また、上記基板３は、当該基板３の表面外周が基板ホルダ４と接触するようにして当該基板ホルダ４と背

板５との間に挟持されている。当該基板ホルダ４は、アルミニウム、ステンレススチール、モリブデン等の導電材で形成されており、基板バイアス電源８に切り替えスイッチ13を介して電気的に接続されている。さらに前記背板５は、加熱ヒータ12が埋め込まれたステンレススチール等からなるテーブル11上に載置されている。また、この例では、金属ターゲット２の直上に複数の固定磁石10を配置しており、また、バルブ６を介して真空槽１内にスパッタガスを供給するようにしている。このスパッタガスとしては、Ar、Kr、Xe等の不活性ガスを適用することができる。

第１図（ｂ）において、本発明を実施するための装置における特徴的な構成が示されている。すなわち当該装置では、基板ホルダ４の基板３外の外周領部分の面積を当該基板３の表面の面積と同程度かまたはそれよりも大きくするようにしている。一例として、外径76mmのSiウエハの全面にＸ線透過膜としてSiN、SiC、BN等が１～４μm厚に形成された基板３を用いた場合、基板ホルダの内径2a（基板３の金属薄膜を形成する部分の直径に同じ）と基板ホルダの外径2bとを、それぞれ74mmと105mmとに設定する。この場合には、基板ホルダ４の外周領部分の表（おもて）面の面積は、基板３の金属薄膜が形成される部分の面積にほぼ等しくなっている。

第２図に、当該装置を用いて、金属ターゲット:Ta、基板直流バイアス電位：浮動（＋６～＋7V）、基板温度:200℃、高周波出力:660W、スパッタガス:Xeガスの条件で、0.7μmのTa膜を形成した場合のXeガス圧力とTa膜応力の関係を示す。同図から、Ta膜応力ゼロ近辺でのスパッタ圧力変化量±0.01Paに対するTa膜応力の変化量は$\pm 0.7\times10^{8}$dyn/cm^{2}であり、Ta膜応力の再現性は同程度であった。

第３図に、スパッタガスとしてXeガスを使用し、その圧力が0.37Pa、高周波出力660W、基板直流バイアス電位が浮動（＋６～＋7V）でTa膜を形成したときの、基板温度とTa膜応力の関係を示す。第３図から、基板温度が高くなるにつれ、Ta膜応力が徐々に高くなることが分かる。また、Ta膜応力を2×10^{8}dyn/cm^{2}以下に制御するためには、基板温度を±５℃程度に制御することが必要であることが分かる。

さらに、第４図に、スパッタガスとしてXeガスを使用し、その圧力が0.37Pa、高周波出力660W、基板温度200℃でTa膜を形成したときの、基板直流バイアス電位とTa膜応力の関係を示す。第４図から、この例では、基板直流バイアス電位が－15V以下ではTa膜応力が急激に圧縮応力となり、不適切であることが分かる。第７図に示した従来例では、基板直流バイアス電位が0V以下で不適切であったので、本発明実施例の第４図では基板直流バイアス電位の適性範囲が広がったことになる。従って、基板直流バイアス電位の制約が緩まり、制御がしやすくなったことを示す。

この例では、適切にガス圧力、スパッタ電力および基盤温度を調整することにより、Ta膜応力が$\pm 1\times10^{9}$dyn/cm^{2}の範囲で$\pm 0.7\times10^{8}$dyn/cm^{2}の精度で膜応力を制御することが可能であった。

なお、以上説明してきた例では円形の基板３および円形の基板ホルダ４を用いたものを取り上げたが、これに限らず、例えば矩形の基板等を適用してもよいことはいうまでもない。

また、マグネトロンスパッタ装置を例として用いたが、他のスパッタ装置を用いてもよい。さらには、スパッタ電源およびバイアス電源は、高周波電源でも直流電源でも、用途に応じて適用することができる。

以上説明したように、本発明の低応力金属薄膜の形成方法によれば、これまで困難であった低応力の金属薄膜を高精度に形成することができる。このため、例えば半導体集積回路の電極パターンの形成に適用した場合には、膜応力等に起因するストレスマイグレーションの少ない半導体集積回路素子を得ることができる。また、Ｘ線露光用マスクの吸収体パターンの形成に適用した場合には、膜応力に起因する吸収体パターンの位置ずれを防止でき、高精度なＸ線露光用マスクを得ることができる。

【図面の簡単な説明】

第１図（ａ）は本発明の低応力金属薄膜の形成方法に適用して好適なスパッタ装置の一実施例の構成を説明するための図、第１図（ｂ）は当該装置における基板と基板ホルダとの関係を説明するための図、第２図は膜応力とXe ガス圧力の関係を示す図、第３図は膜応力と基板温度の関係を示す図、第４図は膜応力と基板直流バイアス電位の関係を示す図、第５図（ａ）は従来技術に係るスパッタ装置の一構成例を示す概念図、第５図（ｂ）は当該装置における基板と基板ホルダの関係を示す図、第６図は膜応力とXe ガス圧力の関係を示す図、第７図は膜応力と基板直流バイアス電位の関係を示す図である。

１……真空槽、２……金属ターゲット、３……基板、４……基板ホルダ、５……背板、６……バルブ、７……スパッタ高周波電源、８……基板バイアス直流電源、９……同調コンデンサ、10……固定磁石、11……テーブル、12……加熱ヒータ、13……切り替えスイッチ。

【第１図（ａ）】

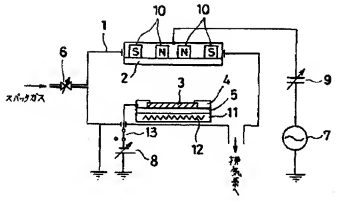

【第１図（ｂ）】

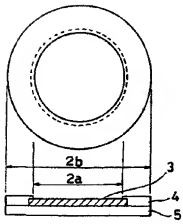

【第２図】

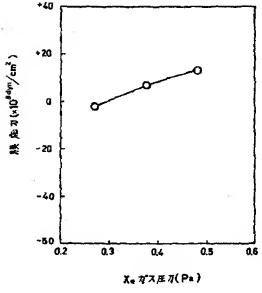

【第３図】

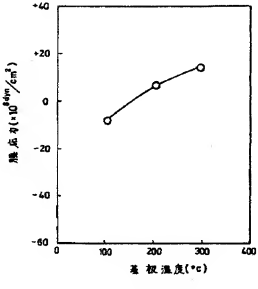

【第５図（ａ）】

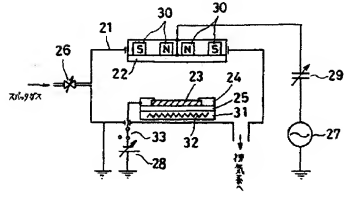

【第５図（ｂ）】

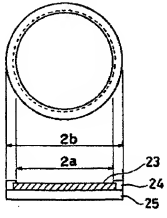

【第４図】

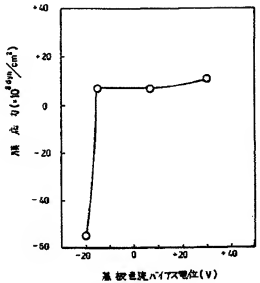

【第６図】（FIG. 6）

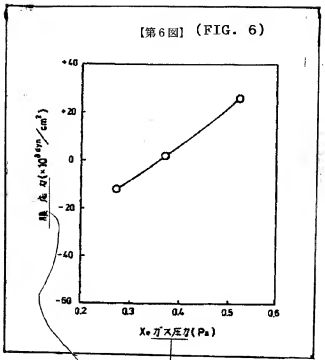

Gas pressure

Accommodate force

【第７図】